The Electronic Spectroscopy and Photophysics of Piperidine in the Vapor Phase

Arthur M. Halpern,* B. R. Ramachandran, and Eric D. Glendening

Department of Chemistry, Indiana State University, Terre Haute, Indiana 47809

Received: August 21, 2000; In Final Form: October 17, 2000

The ground- and lowest excited-state properties of piperidine vapor are explored with respect to understanding its absorption and fluorescence properties. A ground-state intrinsic reaction coordinate (IRC) calculation was used to model the conformational potential energy surface connecting the equatorial and axial conformers. At the MP2/6-311++G** level of theory, the equatorial conformer is more stable by 310 cm^{-1} than the axial conformer, and the inversion barrier height is 2033 cm^{-1}. Two transitions in the UV, with origins of 38 707 and 44 070 cm^{-1} are assigned. The $S_1 \leftarrow S_0$ transition ($f_{obs} \sim 3.2 \times 10^{-3}$) is Rydberg in nature, with considerable involvement of all the ring heavy atoms. A vibrational analysis of this transition shows a main progression in 640 cm^{-1}, which is assigned as the N−H out-of-plane bending motion. The CIS-calculated equilibrium geometry of the S_1 state indicates considerable distortion of the N atom relative to the C_α atoms. The one-dimensional absorption spectrum is modeled on the basis of the ground-state IRC and the corresponding vertical CAS(2,2)/MP2 surface. The IRC dependence of the transition moment was taken into account. The radiative rate constant, k_r, is estimated be ca. 1.7×10^6 s^{-1}. A weak fluorescence with $\tilde{\nu}_{max} = 33\,500$ cm^{-1} is observed with a quantum efficiency, q_f, of ca. 1.3×10^{-4}. The lifetime of the S_1 state is estimated to be ca. 80 ps on the basis of q_f/k_r. Deuterium substitution (*d*1 and *d*11) results in slight increases in q_f.

Introduction

Tertiary saturated amines are highly fluorescent compounds, both in the vapor phase[1] and nonpolar solution[2]. For example, the fluorescence efficiency of the simplest such compound, trimethylamine, has been reported to be near unity if the excitation wavelength is not too short, and the system is fully vibrationally relaxed and does not undergo self-quenching.[1,3] Other tertiary amines, such as triethylamine and *N*-methylpiperidine have similarly high fluorescence efficiencies. Considering the high radiative transition probabilities and relatively weakly allowed, low-lying absorption spectra, the S_1 states of such compounds are moderately long-lived (e.g., gas-phase lifetimes of 61 and 60 ns, respectively), allowing the excited state to be collisionally intercepted, with such consequences as fluorescence quenching,[4] energy transfer,[5] and, in certain cases, excimer[6] and exciplex[5] formation.

An immediate implication of the intrinsically high fluorescence efficiencies and long S_1 lifetimes of these compounds (in the vapor phase and dilute nonpolar solution) is that nonradiative decay from S_1 is slow. This is at first somewhat surprising considering the fact that the $S_1 - S_0$ energy is considerably greater than the N−C bond dissociation energy (i.e., 37 600 and 27 600 cm^{-1}, respectively). It also thus appears that intersystem crossing into the triplet manifold, and internal conversion to the ground state, are also relatively slow (< ca. 10^5 s^{-1}).

For these reasons we were motivated to explore the spectroscopic and photophysical properties of the simple secondary amine, piperidine. Piperidine was chosen because its *N*-methyl derivative is often used as a model tertiary amine in our laboratory in connection with studies of the N−N intramolecular interactions in *N*,*N*′-dimethylpiperazine. We also wanted to study a secondary amine that did not present complications arising from methyl rotations, such as might be the case, for example, in *N*,*N*-dimethylamine.

The immediate objective of this study was to determine the fluorescence efficiency and lifetime of the relaxed S_1 state of piperidine so that we could obtain the total nonradiative relaxation constant, and to compare these results with *N*-methylpiperidine. As a part of these particular studies, we undertook a theoretical investigation of the ground-state conformational energetics of piperidine, and their implications for the electronic absorption spectrum. We also reinvestigated the vapor-phase electronic absorption spectrum of piperidine, and conducted ab initio calculations on the lowest excited singlet state to determine its structure and relevant vibrational modes.

Experimental Section

Piperidine (Aldrich) was refluxed and distilled over CaH_2, and thereafter stored in an evacuated reservoir. *n*-Hexane, (Fisher "Optima"), used as a vibrational relaxation agent, was deaerated using several freeze−pump−thaw cycles, and kept in vacuo. Piperidine-d_1 was prepared by equilibrating piperidine (6.3 g, 0.074 mol) with D_2O (40 g, 2 mol) containing five drops of DCl (20 wt % in D_2O) at 23 °C for 6 days. The solution was made strongly basic using a solution of NaOD (40 wt % in D_2O) and separated into two phases. A volume of 10 mL of the organic-rich phase was extracted with *n*-pentane (spectrograde, Aldrich) using a continuous liquid−liquid extractor for 24 h. The extract was dried over anhydrous Na_2SO_4. The *n*-pentane was removed by fractional distillation (37−43 °C) at ambient pressure. On continued heating, *N*-deuteriopiperidine distilled at 103 °C. The fraction boiling between 105 and 105.5 °C (ca. 5 g) was stored under N_2 in the dark. Spectral (H NMR,

* Author to whom correspondence should be addressed. Fax: (812) 237-2232. E-mail: a-halpern@indstate.edu.

10.1021/jp002990g CCC: $19.00
Published on Web 11/28/2000

IR) and MS analysis of the *N*-deuteriopiperidine revealed an isotopic purity of ca. 97%. Perdeuteriopiperidine (Cambridge Isotope Laboratories) was used without further treatment.

Absorption spectra were acquired using a Cary 5 spectrophotometer configured to have a band-pass of 0.1 nm and to acquire spectra at a constant signal-to-noise ratio of 100−200. Emission spectra were obtained using a Spex Fluorolog with a 200-W Hg(Xe) source from which 238 radiation was isolated. The multiple scan option was used to increase the signal-to-noise ratio; typically 40 scans were run. The emission band-pass was 3.8 nm.

IR spectra were obtained with a Midac FT-IR spectrometer (model M2000). A 10-cm gas cell, fitted with KBr windows was filled with the liquid-equilibrated vapor at 23 °C.

The $S_1 \leftarrow S_0$ transition was resolved from the stronger $S_2 \leftarrow S_0$ transition by fitting a Gaussian function to the portion of the observed spectrum between 47 590 and 49 830 cm^{-1}. We used that function to represent $S_2 \leftarrow S_0$ band, which was then subtracted from the observed spectrum at lower energies to isolate the low-energy part of the $S_1 \leftarrow S_0$ absorption. We then approximated the full $S_1 \leftarrow S_0$ absorption spectrum by reflecting the low-energy curve about its maximum at ca. 43 100 cm^{-1}. The $S_2 \leftarrow S_0$ absorption spectrum was then obtained by subtracting the $S_1 \leftarrow S_0$ spectrum from the observed spectrum. The oscillator strengths, *f*, of the $S_1 \leftarrow S_0$ and $S_2 \leftarrow S_0$ transitions were obtained from

$$f = 4.32 \times 10^{-9} \int_{\text{band}} \epsilon \, d\tilde{\nu} \qquad (1)$$

where $\epsilon(\tilde{\nu})$ is the molar absorbtivity. The radiative rate constant, k_r, was approximated from the relation[7]

$$k_r = 2.88 \times 10^{-9} \langle \tilde{\nu}_f^{-3} \rangle^{-1} \int_{S_1 \leftarrow S_0} \frac{\epsilon(\tilde{\nu})\, d\tilde{\nu}}{\tilde{\nu}} \qquad (2)$$

where $\langle \tilde{\nu}_f^{-3} \rangle$ is the mean reciprocal cube of the fluorescence frequency. The integration is over the $S_1 \leftarrow S_0$ band.

Calculations were performed using Gaussian 98[8] and MOLPRO.[9]

Results and Discussion

1. Ground State Conformational Structure. Although the main focus of this paper is on the photophysics of piperidine vapor, with an emphasis on the properties of the S_1 state, we begin the discussion by giving some attention to the ground state. This is necessary in view of the fact that, as we will indicate, the equilibrium structure of the relaxed S_1 state is planar with respect to the N-atom center, in contrast to the pyramidal ground-state conformers. It is important, therefore, to understand the potential energy surface of the equatorial and axial conformers of ground-state piperidine in connection with its absorption and emission spectra. Thus we must, in principle, deal with these two absorbing conformers, which presumably have a common excited state. Furthermore, as we will show, the absorption probability of the axial conformer is calculated to be larger than that of the equatorial conformer.

To determine the relative energetics of these conformers we fully optimized the respective structures at the MP2 level of theory using the 6-311++G** basis set. These calculations indicate that, as expected,[10,11] the equatorial conformer (**I**) is more stable—in this calculation by 301 cm^{-1}—than the axial structure (**II**). In addition, a QST2 calculation located the inversion transition state (**III**), which is calculated to lie 2033 cm^{-1} above the equatorial conformer. From these results we estimate that ca. 75% of piperidine molecules are in the equatorial conformation at 300 K, assuming thermal equilibrium between the conformers.

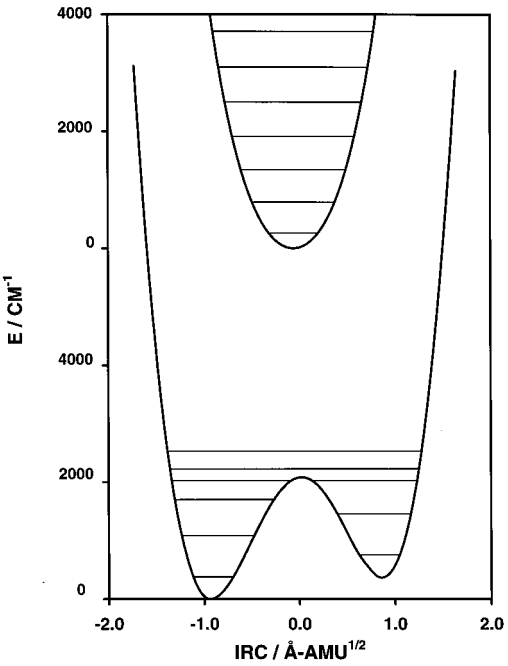

Figure 1. IRC potentials and eigenvalues of the S_0 and S_1 states of piperidine. The fully relaxed S_0 potential is obtained from an IRC MP2/6-31+G* calculation, and the S_1 vertical potential is obtained from single-point CAS(2,2)/6-31+G* MP2 calculations.

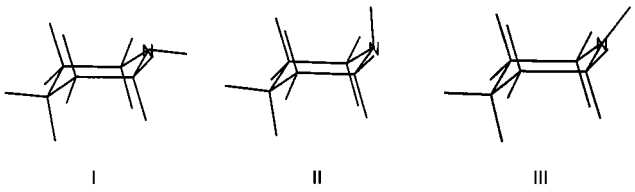

We examined more fully the energetics of N-inversion in ground-state piperidine. Accordingly, we performed an intrinsic reaction coordinate (IRC) calculation[12] of the inversion motion. A significant feature of this calculation is that, unlike a relaxed potential energy surface scan based on a single internal coordinate, it utilizes a mass-weighted reaction coordinate, which obviates the need to develop a model for the effective reduced mass (or account for the coordinate dependence of the reduced mass) in determining the eigenvalues associated with the IRC potential. This potential, obtained at the MP2/6-31+G* level of theory, is shown in Figure 1, along with its eigenvalues. These eigenvalues can be compared with the calculated (harmonic) frequencies associated with the inversion motion of the two conformers. From an MP2/6-31+G* calculation, these values (for ν_7, a strongly IR-allowed transition) are 801.7 and 792.3 cm^{-1} for the equatorial and axial conformers, respectively. The IRC potential gives fundamental frequencies of 691 and 683 cm^{-1} for these conformers, respectively, which, considering the strongly anharmonic quality of the inversion potential, are predictably smaller than the MP2-calculated values. Interestingly, the differences between the ν_7 values of the equatorial and axial conformers are similar for the MP2 and IRC calculations, i.e., 9.5 and 7.1 cm^{-1}, respectively. The IR spectrum of piperidine vapor shows a strong set of poorly resolved bands in the 720−750 cm^{-1} region in which we discern two overlapping bands centered at 738.0 and 727.2 cm^{-1}, which may be

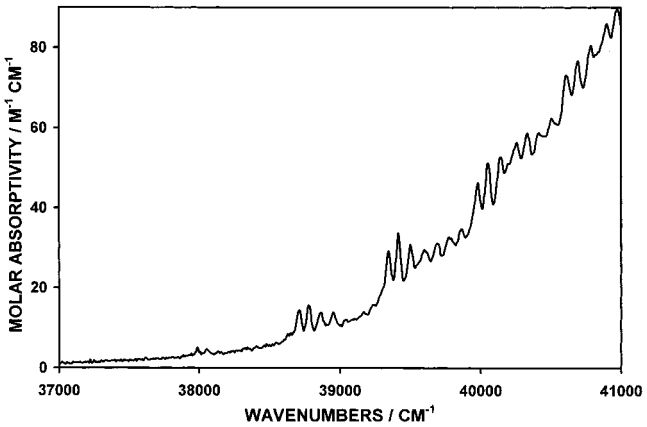

Figure 2. The absorption spectrum of piperidine vapor at 296 K obtained at a bandwidth of ca. 16 cm^{-1}.

associated with the equatorial and axial conformers. Vedal et al. have also reported (and depicted graphically) a complex set of bands in piperidine vapor in this region.[13] From the relative intensities of the 738 and 727 cm^{-1} bands, we estimate the axial−equatorial energy difference to be approximately 175 cm^{-1}. This result compares with our MP2 value of 301 cm^{-1} (see above) and with literature values of 175 cm^{-1} (IR),[14] 140 (dipole moment),[15] 260 cm^{-1} (microwave),[16] and 126 cm^{-1} (NMR).[17]

The conformational inversion barrier obtained from these IRC calculations is 2075 cm^{-1}, which is very close to the value of 2033 cm^{-1} cited above for the QST2 results. An interesting characteristic of the transition state structure (**III**) is that the N,H,C$_\alpha$,C′$_\alpha$ atoms are not exactly coplanar, i.e., the H atom lies ca. 5° out of the N,C$_\alpha$,C′$_\alpha$ plane.

2. Electronic Absorption Spectrum. We acquired the absorption spectrum of piperidine vapor at 296 K at moderate resolution (ca. 16 cm^{-1}) between 36 000 and 52 000 cm^{-1}. Two absorption systems can be identified in this region: a weakly allowed transition commencing at ca. 38 800 cm^{-1} with an oscillator strength, *f*, of ca. 3.2 × 10^{-3} and a more strongly allowed system beginning at ca. 44 000 cm^{-1} having an estimated *f* value of ca. 0.06 (see Experimental Section). We attribute these absorptions to the $S_1 \leftarrow S_0$ and $S_2 \leftarrow S_0$ transitions, respectively. The $S_1 \leftarrow S_0$ transition is considerably distorted by the low-energy tail of the more intense $S_2 \leftarrow S_0$ transition, but nevertheless displays considerable vibronic structure. Figure 2 displays the spectrum between 37 000 and 41 000 cm^{-1}. We assign the feature at 38 707 cm^{-1} as the 0−0 band. Nath et al.[18] also attributed this feature (reported by them at 38 731) as the transition origin. At least five members of a progression in ca. 640 cm^{-1} can be seen to arise from the 0−0 band, and the mode associated with this progression appears to be quite harmonic (spacings between the progression members are constant within ca. 8 cm^{-1}). A set of features at ca. 38 000 cm^{-1} appears to be hot bands, the displacement of which is ca. 720 cm^{-1} to the red of the 0−0 band. The principal feature here at 37 987 cm^{-1} is approximately 0.26 as intense as the 0−0 band. Although this is an order of magnitude larger than would be expected on the basis of the Boltzmann factor, it is possible that the increased Franck−Condon factor of this mode, or possibly the transition matrix element, enhances the transition probability. Another possibility, however, is that the 37 987 cm^{-1} feature is actually the origin and the 38 707 cm^{-1} transition is the first of a 720 cm^{-1} progression, with the other five features being members of a 640 cm^{-1} progression built off of the 38 707 cm^{-1} absorption band.

We studied the temperature dependence of the absorption spectrum in this region between 282 and 313 K. Over this temperature range the intensity of the 37 987 cm^{-1} band increased by a factor of ca. 1.7 relative to the 38 707 cm^{-1} band. This Boltzmann factor is consistent with the energy separation of these bands of 720 cm^{-1}, and appears to confirm that the 37 987 cm^{-1} features are thermal in origin, and also indicates that none of the four prominent features at 38 707 cm^{-1} are hot bands or sequences. Thus we remain with our assignment of the 38 707 cm^{-1} feature as being the 0−0 band of the $S_1 \leftarrow S_0$ transition.

As shown in Figure 2, the cluster of features at ca. 38 800 cm^{-1} (including the 0−0 band) contains several closely separated components with cumulative spacings of 68, 158, 241, and 333 cm^{-1}. This pattern seems to be repeated for the first three members of the 640 cm^{-1} progression, as well as for the hot band. Nath et al.[18] have reported three frequencies (91, 176, and 646 cm^{-1}) in the pipridine spectrum. Our value of the 68 cm^{-1} separation between the 0−0 band and the next prominent feature differs from theirs, which was determined from photographic data. Because of the temperature independence of the intensities of these bands, we assign the three main bands to the blue of the 0−0 band as members of one, or possibly two, low-frequency progressions.

A CIS frequency calculation of the optimized S_1 state (**IV**) of piperidine indicates that the lowest-frequency mode in that state is 150 cm^{-1}, and corresponds to a mode having considerable N-atom out-of-plane bending character. This activity is likely to be very important in coupling the S_0 and S_1 states because the CIS-optimized geometry of the latter is very distorted with respect to the position of the N atom vis-à-vis the ground state. This significant geometry change is indicated in **IV**. It is noticeable that it is principally the N atom itself, rather than the H(N) atom, that is displaced in the relaxed S_1 state.

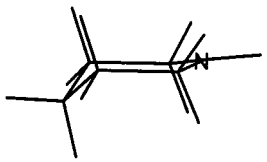

IV

Anticipating that the N atom is in a (nearly) planar arrangement in the equilibrium S_1 state, we may expect the ground state N-bending motion to be strongly coupled with the $S_1 \leftarrow S_0$ transition. It is therefore reasonable to assign the 720 cm^{-1} hot band to the N-bending mode of the (principally equatorial) ground state, and the 640 cm^{-1} progression to excitation of the N-atom out-of-plane bending mode of S_1. We will discuss the structural and vibrational properties of the S_1 state in the next section.

The UV absorption spectrum of piperidine up to 50 000 cm^{-1} is shown in Figure 3. We attempted to decompose the total absorption (A) into its $S_1 \leftarrow S_0$ and $S_2 \leftarrow S_0$ components (see Experimental Section). On this basis we estimate the vertical $S_1 \leftarrow S_0$ transition energy to be ca. 43 100 cm^{-1}. We assign the origin of the more intensely allowed $S_2 \leftarrow S_0$ transition at 44 070 cm^{-1}. Several vibrational features are observed in this spectrum and may be interpreted in terms of possibly two progressions in ca. 630 cm^{-1} and a single member of a 735 cm^{-1} progression; however, the spectrum, is too diffuse in this region to warrant further analysis.

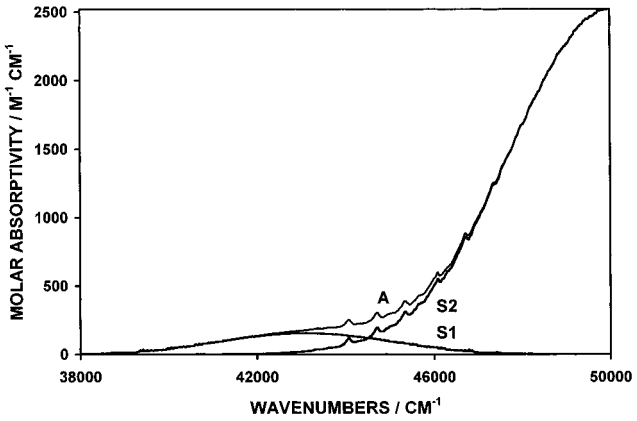

Figure 3. The decomposition of the absorption spectrum of piperidine vapor at 296 K (A) into its $S_1 \leftarrow S_0$ (S1) and $S_2 \leftarrow S_0$ (S2) components. (See Experimental Section.)

3. The S_1 State

The CIS/6-31+G* calculation of the equatorial conformer places the vertical S_1 state at 56 000 cm^{-1} with an oscillator strength, *f*, of 0.0008. The same calculation of the axial conformer locates the vertical S_1 state at 56 350 cm^{-1} (f = 0.015). Although the experimental vertical transition energy cannot be directly determined because of the interference of the more strongly allowed $S_2 \leftarrow S_0$ transition, these CIS values are clearly much too high. A natural bond orbital[19] (NBO) analysis of the CIS (equatorial) results for the $S_1 \leftarrow S_0$ transition indicates that it corresponds to the promotion of an electron from the HOMO, which is principally the n_N orbital (70%) but with appreciable contribution from the two anti $C_\alpha-H$ bonds (17%), to an extensively delocalized molecular Rydberg orbital. The CIS calculation indicates that the largest contribution to the $S_1 \leftarrow S_0$ transition is the HOMO $\rightarrow$ LUMO promotion (35%), with the latter m.o. consisting of Rydberg orbitals on the α-C atoms (29%) and the N atom (10%), with the remaining density delocalized over other atomic centers. The other virtual orbitals that are involved in the S_1 state also consist of Rydberg orbitals centered on *all* the heavy atoms. These calculations reinforce the concept that the excited states of the saturated amines are very diffuse[20,21] and, in the case of piperidine, involve nearly the entire heavy-atom framework.

As mentioned above, and as shown in **IV** vis-à-vis **I** and **II**, the relaxed S_1 state of piperidine is very distorted relative to the ground-state conformers, particularly with respect to the positions of the N and H atoms. For example, in the S_1 state the $C'-N-C_\alpha-C_\beta$ dihedral angle is 17.5°, whereas it is 30.1° in the ground (equatorial) state. Also, the N atom in the S_1 state is nearly planar: the $C_\alpha-N-C'_\alpha$ and $C_\alpha-N-H$ bond angles are 127.4° and 115.9°, respectively (the sum of the central bond angles on the N atom is 359.2°). It is interesting to note that the S_1 N−H bond length is slightly longer than that in S_0, i.e., 1.044 and 1.020 Å, respectively. The 0−0 energy of the $S_1 \leftarrow S_0$ transition (zero-point energy-corrected) obtained from the CIS/6-31+G* calculation is 47 700 cm^{-1}, which compares with our assigned value of 38 707 cm^{-1}. Again we see that the CIS method, along with the relatively restricted basis set used, considerably overestimates the transition energy.

We further explored the S_1 surface by calculating the vertical S_1 surface reached from points along the ground-state IRC. This surface was obtained by performing CAS(2,2)MP2/6-31+G* single-point calculations on piperidine structures along the ground-state IRC described in Section 1. The S_1 surface and the eigenvalues thus obtained are shown along with the relaxed ground-state IRC in Figure 1. The eigenfunctions and eigenvectors associated with these IRC surfaces were used to construct the corresponding one-dimensional absorption spectrum. Because the electronic transition matrix element is dependent on the IRC coordinate (the axial conformer having a larger $S_1 \leftarrow S_0$ transition moment), the vibronic components of the spectrum were obtained from the vibrational transition moment matrix elements using the relationship[22]

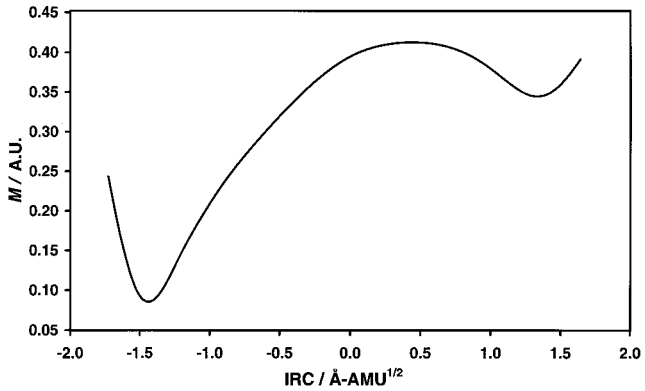

Figure 4. The IRC dependence of the electronic transition matrix element, *M*, of piperidine.

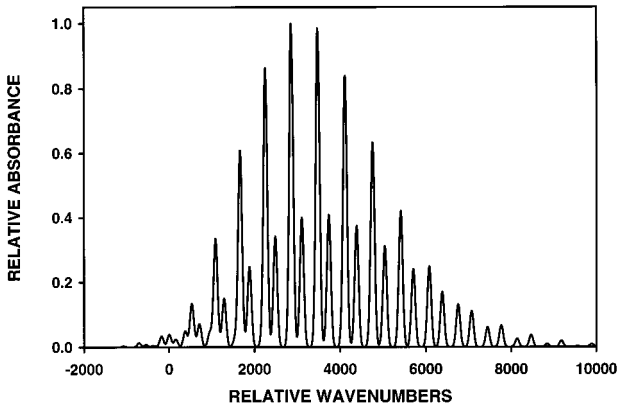

Figure 5. One-dimensional absorption spectrum of piperidine modeled from the IRC surfaces shown in Figure 1. The IRC dependence of the electronic transition moment is taken into account using eq 3. Each "stick" is Gaussian broadened by 120 cm^{-1}.

$$I_{v'',v'} \propto N_{v''} \tilde{\nu}_{v'',v'} [\int \Psi_{v''}^{S_0} M(Q) \Psi_{v'}^{S_1} \, dQ]^2 \qquad (3)$$

where $N_{v''}$ is the Boltzmann factor of the v″th eigenstate of the S_0 state, $\tilde{\nu}_{v'',v'}$ is the frequency of the vibronic transition, the ψ's are the vibrational wave functions of the S_0 and S_1 states, and $M(Q)$ represents the IRC coordinate-dependent electronic transition moment. A plot of $M(Q)$ is shown in Figure 4 and indicates the intrinsically larger $S_1 \leftarrow S_0$ absorption probability for axial-like conformations of piperidine.

The calculated absorption spectrum modeled on the IRC surfaces shown in Figure 1 is depicted in Figure 5. This spectrum cannot be directly compared with the experimental spectrum (Figure 2), not only because the profile of the latter is considerably distorted by the more strongly allowed $S_2 \leftarrow S_0$ spectrum, but also because it is by nature one-dimensional, while the experimental one undoubtedly represents several vibrational modes. Nevertheless, it is evident that one expects essentially a superposition of absorption spectra arising from the two conformers, offset from each other by the difference in zero-point energies of the conformers. Some general patterns seen in the calculated spectrum that can be recognized in the

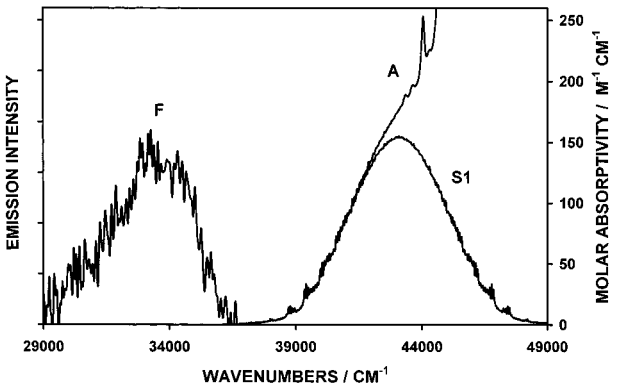

Figure 6. The fluorescence spectrum (F) of piperidine vapor excited at 228 nm and 296 K in the presence of 100 Torr of hexane. The observed absorption spectrum (A) and the estimated $S_1 \leftarrow S_0$ spectrum are also shown. The feature in (A) at 44 070 cm^{-1} is assigned as the 0−0 band of the $S_2 \leftarrow S_0$ transition.

experimental spectrum such as (1) the prominent progression in what might be characterized as the upper state out-of-plane bending motion (i.e., $\tilde{\nu}_{obs} = 640$ cm^{-1}; $\tilde{\nu}_{calc} = 540$ cm^{-1}) and (2) the clustering of bands that, in the case of the calculated spectrum, arise from transitions from the two conformers. In the latter situation, however, the observed spacing is much smaller than that calculated (i.e., 60−90 cm^{-1} observed; 190−230 cm^{-1} calculated). The calculated spectrum shows that despite the IRC-dependence of the transition moment, as well as the displacement between the S_0 and S_1 along the IRC, the transition origin (at "0" energy) is discernible, although weak.

Fluorescence Spectrum. Piperidine vapor (15 Torr), when irradiated at 238 nm (42 000 cm^{-1}) produces a weak, seemingly structureless emission band centered at 33500 cm^{-1}. Although one must be very cautious about making assignments of weak emission, especially in view of the fact that in this case there are no definitive, i.e., vibronic, features, we attribute the 33 500 cm^{-1} band to the $S_1 \rightarrow S_0$ fluorescence of piperidine. This emission spectrum is shown in Figure 6 along with the Franck−Condon profile of the $S_1 \leftarrow S_0$ spectrum that we decomposed from the total absorbance (see Figure 3). The Stokes's shift is estimated to be ca. 9600 cm^{-1}.

We note that the emission intensity was proportional to the piperidine pressure used to fill the cell, and we are reasonably confident of the purity of the piperidine used in our experiments. We also point out that the signal strength was time independent, the intensity remaining constant after ∼1 h of irradiation suggesting that piperidine is photostable under our experimental conditions.

Given the highly distorted structure obtained from the CIS-optimized S_1 state vis-à-vis the ground state (see I and IV), we can anticipate that the corresponding Franck−Condon ground state produced via radiative relaxation from S_1 will be fairly energetic, possessing both considerable ring strain as well as N-atom rehybridizing energy. Indeed, the observed red shift of the piperidine fluorescence maximum relative to the 0−0 band of the $S_1 \leftarrow S_0$ transition, is ca. 4,500 cm^{-1}. This value can be compared with the calculated energy difference of 4,900 cm^{-1} between a RHF/6-31+G* energy of the S_1 state at the optimal geometry (i.e., the Franck−Condon state reached via fluorescence) and that of the equilibrium equatorial geometry. It should be noted, however, that the observed fluorescence might not be fully collisionally relaxed (see below).

The fluorescence quantum efficiency of the piperidine emission, q_f, is estimated to be 1.3×10^{-4} ($\sigma = 0.1 \times 10^{-4}$), based on a value of 0.98 for *N*-methylpiperidine vapor.[1] In an attempt to achieve vibrational relaxation in the S_1 manifold, piperidine fluorescence was obtained in the presence of ca. 100 Torr of *n*-hexane (the excitation energy used is ca. 3300 cm^{-1} above the 0−0 band of the $S_1 \leftarrow S_0$ transition). We were unable to determine the fluorescence lifetime of piperidine because of its weakness and also its presumed very fast decay. However, using the estimated oscillator strength of the $S_1 \leftarrow S_0$ transition along with $\tilde{\nu}_{max}$ of the fluorescence spectrum, we estimated the corresponding radiative rate constant, k_r, to be ca. 1.7×10^6 s^{-1}. This value allows us to obtain an estimate of the fluorescence lifetime, τ_f, of ∼80 ps (i.e., a decay rate of 1.3×10^{10} s^{-1}), based on the relationship $\tau_f = q_f/k_r$. Because of its presumably very short lifetime, the piperidine S_1 state is probably not completely vibrationally relaxed in our experiments where the total pressure is only ca. 115 Torr. At this pressure the collision frequency is only ca. 1.2×10^9 s^{-1}. A pressure of ca. 16 atm of buffer gas would be required to provide a collision frequency equal to the piperidine S_1 decay rate. Thus we believe that the measured fluorescence efficiency represents a lower limit, assuming that vibrational relaxation in the S_1 manifold would result in fluorescence enhancement, a result of the generally expected decrease in the nonradiative decay rate with decreasing vibrational energy. Table 1 summarizes the photophysical and spectroscopic data reported here for piperidine vapor.

TABLE 1: Summary of Spectroscopic and Photophysical Data for Piperidine Vapor at 296 K

$S_1 \leftarrow S_0$ (0,0)	38 708 cm^{-1} (258.34 nm)
$S_2 \leftarrow S_0$ (0,0)	44 070 cm^{-1} (226.91 nm)
$S_1 \leftarrow S_0$ (vert)[a]	43 100 cm^{-1} (232 nm)
$S_1 \rightarrow S_0$ (vert)	33 500 cm^{-1} (299 nm)
$f_{S_1 \leftarrow S_0}$[a,b]	0.003
$f_{S_2 \leftarrow S_0}$[a,b]	0.06
q_f	1.3×10^{-4}
k_r[c]	1.7×10^6 s^{-1}
τ_f[d]	80 ps

[a] Estimated by separating the observed absorption into the $S_1 \leftarrow S_0$ and $S_2 \leftarrow S_0$ components. [b] Calculated using eq 1. [c] Calculated using eq 2. [d] Obtained from q_f/k_r.

The immediate question posed by these results is why radiationless decay in piperidine vapor is so much faster than that in *N*-methylpiperidine, i.e., ca. 1.3×10^{10} s^{-1} compared with 3.3×10^5 s^{-1}. It is not known at this time which nonradiative process (or processes) depletes the S_1 state of piperidine, or, for that matter, any of the saturated secondary amines in general. Initial studies in our laboratory indicate that dimethylamine vapor fluoresces with a very small quantum efficiency. As mentioned above, qualitative data indicate that vapor-phase piperidine appears to be relatively photostable, i.e., the weak fluorescence signal observed does not decrease upon prolonged irradiation at 238 nm. Thus it is perhaps unlikely that the S_1 state is effectively depleted via photodissociation. Because the triplet states of these compounds have not been identified yet, it is premature to speculate about the possible enhanced rate of intersystem crossing in secondary vis-à-vis tertiary amines.

To explore the possibility that the N−H stretching mode (or other related vibration) is involved in radiationless decay in piperidine, we determined the fluorescence quantum efficiencies of piperidine-*d*1 and perdeuteriopiperidine under identical conditions as those for piperidine as reported above. The results indicate only very small increases in q_f for piperidine-d_1 and

perdeuteriopiperidine, i.e., 1.6×10^{-4} ($\sigma = 0.3 \times 10^{-4}$) and 4.3×10^{-4} ($\sigma = 0.5 \times 10^{-4}$), respectively (cf. 1.3×10^{-4} for piperidine). Assuming that the radiative rate constant of piperidine is unaffected by deuteration, these data suggest that there is a slight decrease in the nonradiative decay rate from the S_1 state of the deuterated compounds, presumably as a consequence of lower vibrational frequencies and their effect on Franck−Condon factors or tunneling rates. There seems to be no implication that motion involving the N−H atom is particularly significant in promoting nonradiative decay. Further studies of the photophysics of secondary amines are continuing.

Acknowledgment. We thank Cambridge Isotope Laboratories, Inc., for a sample of piperidine-d_{11}.

References and Notes

(1) Halpern, A. M.; Gartman, T. *J. Am. Chem. Soc.* **1974**, *96*, 1393.
(2) Halpern, A. M.; Wong, D. K. *Chem. Phys. Lett.* **1976**, *37*, 416.
(3) Halpern, A. M.; Ondrechen, M. J.; Ziegler, L. D. *J. Am. Chem. Soc.* **1986**, *108*, 3907.
(4) Halpern, A. M.; Wryzykowska, K. *J. Photochem.* **1981**, *15*, 147.
(5) Halpern, A. M.; Wryzykowska, K. *Chem. Phys. Lett.* **1981**, *77*, 82.
(6) Halpern, A. M.; Ravinet, P.; Sternfels, R. J. *J. Am. Chem. Soc.* **1977**, *99*, 169.
(7) Birks, J. B. *Photophysics of Aromatic Molecules*; Wiley-Interscience: London, 1970; p 88.
(8) Frisch, M. J.; Trucks, G. W.; Schlegel, H. B.; Scuseria, G. E.; Robb, M. A.; Cheeseman, J. R.; Zakrzewski, V. G.; Montgomery, J. A., Jr.; Stratmann, R. E.; Burant, J. C.; Dapprich, S.; Millam, J. M.; Daniels, A. D.; Kudin, K. N.; Strain, M. C.; Farkas, O.; Tomasi, J.; Barone, V.; Cossi, M.; Cammi, R.; Mennucci, B.; Pomelli, C.; Adamo, C.; Clifford, S.; Ochterski, J.; Petersson, G. A.; Ayala, P. Y.; Cui, Q.; Morokuma, K.; Malick, D. K.; Rabuck, A. D.; Raghavachari, K.; Foresman, J. B.; Cioslowski, J.; Ortiz, J. V.; Baboul, A. G.; Stefanov, B. B.; Liu, G.; Liashenko, A.; Piskorz, P.; Komaromi, I.; Gomperts, R.; Martin, R. L.; Fox, D. J.; Keith, T.; Al-Laham, M. A.; Peng, C. Y.; Nanayakkara, A.; Gonzalez, C.; Challacombe, M.; Gill, P. M. W.; Johnson, B.; Chen, W.; Wong, M. W.; Andres, J. L.; Gonzalez, C.; Head-Gordon, M.; Replogle, E. S.; Pople, J. A. *Gaussian 98*, Revision A.7; Gaussian, Inc.: Pittsburgh, PA, 1998.
(9) MOLPRO is a package of ab initio programs written by Werner, H.-J.; Knowles, P. J.; with contributions from Almlöf, J.; Amos, R. D.; Berning, A.; Cooper, D. L.; Degan, M. J. O.; Dobbyn, A. J.; Eckert, F.; Hampel, C.; Lindh, R.; Lloyd, A. W.; Meyet, W.; Nicklass, A.; Peterson, K.; Pitzer, R.; Stone, A. J.; Taylor, P. R.; Mura, M. E.; Pulay, P.; Schütz, M.; Stoll, H.; Thorsteinsson, T.
(10) Blackburne, I. D.; Katritzky, A. R.; Takeuchi, Y. *Acc. Chem. Res.* **1975**, *8*, 300.
(11) Ladika, M.; Rondan, N. G. *J. Mol. Struct.* (*THEOCHEM*) **1996**, *365*, 21.
(12) Fukui, K. *Acc. Chem. Res*. **1981**, *14*, 363.
(13) Vedal, D.; Ellestad, O. H.; Klaboe, P.; Hagen, G. *Spec. Acta* **1976**, *32A*, 877.
(14) Baldock, R. W.; Katritsky, A. R. *J. Chem. Soc. B* **1968**, 1470.
(15) Jones, R. A. Y.; Katritzsky, A. R.; Richards, A. G.; Wyatt, R. J.; Bishop, R. J.; Sutton, L. E. *J. Chem. Soc. B* **1970**, 127.
(16) Parkin, J. E.; Buckley, P. J.; Costain, C. C. *J. Mol. Spectrosc*. **1981**, *89*, 465.
(17) Anet, F. A. L.; Yaveri, I. *J. Am. Chem. Soc.* **1977**, *99*, 2794.
(18) Nath, S.; Baruah, G. D.; Singh, R. S. S. *Indian J. Pure Appl. Phys*. **1972**, *10*, 490.
(19) Glendening, E. D.; Badenhoop, J. K.; Reed, A. E.; Carpenter, J. E.; Weinhold, F. NBO 4.M, Theoretical Chemistry Institute, University of Wisconsin, Madison, WI, 2000.
(20) Taylor, D. P.; Bernstein, E. R. *J. Chem. Phys.* **1995**, *103*, 10453.
(21) Taylor, D. P.; Dion, C. F.; Bernstein, E. R. *J. Chem. Phys.* **1997**, *105*, 3512.
(22) Herzberg, G. *Molecular Spectra and Molecular Structure, Vol. I., Spectra of Diatomic Molecules*; Van Nostrand: New York, 1950; pp 382−383.